# Split Ring Resonator Loaded Baffles for Decoupling of Dual-polarized Base Station Array

Li, Mengting; Chen, Xiaoming; Zhang, Anxue; Fan, Wei; Kishk, Ahmed

*Published in:*
I E E E Antennas and Wireless Propagation Letters

*DOI (link to publication from Publisher):*
10.1109/LAWP.2020.3020855

*Publication date:*
2020

*Document Version*
Accepted author manuscript, peer reviewed version

# Split Ring Resonator Loaded Baffles for Decoupling of Dual-polarized Base Station Array

Mengting Li, Xiaoming Chen, *Senior Member, IEEE*, Anxue Zhang, Wei Fan, Ahmed A. Kishk, *Life Fellow, IEEE*

***Abstract*—Baffles loaded by split-ring resonator (SRR) are proposed to reduce the mutual coupling for ± 45° dual-polarized multiple-input-multiple-output (MIMO) antenna. Each baffle consists of two rectangular SRR printed on one side of a 1-mm FR4 substrate. The final decoupling structure contains four baffles forming a barrier wall that reduces the coupling over the 5G band of 3.4-3.8 GHz. Dual-polarized cross-dipole array with SRR loading baffles is simulated and measured to demonstrate their effectiveness in the coupling reduction. The results show that the mutual coupling can be effectively reduced below -25 dB over the entire bandwidth while maintaining a compact array.**

***Index Terms*—Decoupling, dual-polarized, MIMO antenna.**

## I. Introduction

MIMO technology continues to be one of the most critical technologies in 5G communications [1]. It was developed into massive MIMO technology employing dozens of antennas in a base station to enhance the data throughput. As the number of antenna units increases, the mutual coupling effect became more prominent. The strong mutual coupling can generate some severe issues, such as increased voltage standing wave ratio (VSWR) [2] and out of band (OOB) emission in the presence of power amplifiers [3]. Usually, the mutual coupling is required to be smaller than -25 dB in order to have negligible effects on the massive MIMO array performance [2], [4].

Many efforts were made to reduce mutual coupling in the literature. The decoupling methods can be roughly classified into several types according to their working principles. The first type introduced another coupling path to counteract the original coupling path. For example, the decoupling ground (DG) method [4] was proposed to cancel the free-space coupling by introducing an out-of-phase surface coupling. Unfortunately, the method was mainly suitable for microstrip arrays instead of realistic base station (BS) arrays [5], [6], [7]. The array decoupling surface (ADS) [2] was proposed for dual-polarized BS array. However, it inevitably increased the profile of the array. The second type changed the coupling mode to orthogonal polarization [8], [9] or transformed the propagation coupling waves into evanescent waves by using a single negative permeability metasurface [10], [11]. However, these methods were not suitable for dual-polarized BS arrays. Other decoupling techniques included defected ground plane structures [12], [13], electromagnetic band-gap (EBG) [14], [15], metasurface [16], topology optimization [17], and asymmetrical coplanar strip walls [18], which served as band-stop filters to block the coupling waves. These structures were mainly designed for two-element array and were not suitable for BS arrays.

In this article, decoupling baffles loaded by split-ring resonators (SRR) are proposed to achieve high isolation for a dual-polarized BS array. It works as a bandstop filter that can efficiently suppress the free space coupling for both the co-polarizations and cross-polarization between the dual-polarized array elements. Here, a 1×4 dual-polarized cross-dipole array with SRR-loaded decoupling baffles is simulated and measured as an example to verify the concept. The measured results show that all the mutual coupling is reduced below -25 dB over the 5G band of 3.4-3.8 GHz while maintaining a compact array. Note that the decoupling baffles can also be applied to planar BS arrays. Nevertheless, due to page limitation, the corresponding results are omitted here.

TABLE I PERFORMANCES COMPARISON

| Ref. | array config | center-to-center distance | mutual coup. (dB) | Bandwidth (GHz) | profile height |
|---|---|---|---|---|---|
| [2] | 2×2 | $0.53\lambda_0$ | ≤-25 | 3.3-3.8 (-15dB) | $0.3\lambda_0$ |
| [4] | 2×2 | $0.62\lambda_0$ | ≤-25 | 4.8-5.2 (-10dB) | $0.22\lambda_0$ |
| | 4×4 | $0.62\lambda_0$ | ≤ -24.5 | 4.8-5.2 (-10dB) | $0.25\lambda_0$ |
| [19] | 2×2 | $0.5\lambda_0$ | ≤-20 | 2.4-2.5 (-10dB) | $0.045\lambda_0$ |
| Present | 1×4 | $0.5\lambda_0$ | ≤ -25 | 3.4-3.8 (-15dB) | $0.18\lambda_0$ |

A comparison between this work and recently reported decoupling works for dual-polarized MIMO antenna are summarized in Table I. Arrays in [2] and [4] achieve significant decoupling performance with the worst coupling below -25 dB. However, in [2], the antenna profile increased, and in [4], bandwidth was narrow. The transmission-line based technique [19] also has a very narrow bandwidth. Recently, the

This work was supported in part by the National Natural Science Foundation of China under Grants 61801366 and the Natural Science Foundation of Shaanxi Province under Grant 2020JM-078. (*Corresponding authors: Xiaoming Chen, Anxue Zhang*)

M. Li, X. Chen, and A. Zhang are with the School of Information and Communications Engineering, Xi'an Jiaotong University, Xi'an 710049, China (email: xiaoming.chen@mail.xjtu.edu.cn; anxuezhang@xjtu.edu.cn).

W. Fan is with the Antennas, Propagation and Radio Networking section at the Department of Electronic Systems, Aalborg University, Aalborg 9000, Denmark (email: wfa@es.aau.dk).

A. A. Kishk is with Department of Electrical and Computer Engineering, Concordia University, Montreal, Canada (email: kishk@encs.concordia.ca).

This article has been accepted for publication in a future issue of this journal, but has not been fully edited. Content may change prior to final publication. Citation information: DOI 10.1109/LAWP.2020.3020855, IEEE Antennas and Wireless Propagation Letters



decoupling metasurface superstrate [10], [11] has been successfully applied to large arrays [20]. However, it is confined to narrowband single-polarized arrays. Compared to the literature, the proposed decoupling structure has the following merits: 1) it can be applied to broadband dual-polarized arrays, as opposed to [10], [11], [20]; 2) it has nearly half of the profile as compared to [2] with similar decoupling performances; it achieves good matching (S11 < -15 dB) and decoupilng (measured mutual coupling below -25 dB) performances in the 5G band of 3.4-3.8 GHz.

## II. Decoupling Baffle Loaded by SRR

The configuration of the proposed decoupling baffle is shown in Fig. 1. Two rectangular (metal) SRRs are etched on a 1-mm thick FR4 substrate (with a relative permittivity of 4.4 and a loss tangent of 0.02). A single SRR has a band-gap whose center frequency can be determined from the equivalent inductance $L$ and capacitance $C$ of the structure as [21]

$$f_c = 1/2\pi\sqrt{LC} \tag{1}$$

The inductance $L$ is related to the width and height of the SRR, and the capacitance $C$ is strictly relevant to the value of $t$ and $d2$. A ±45° dual-polarized dipole antenna with compact dimensions is selected as an array element. Details of the unit element design (cf. Fig. 2 (a)) can be found in [22]. Fig. 2 (c) shows the configuration of the antenna unit with the proposed SRR-loaded baffles.

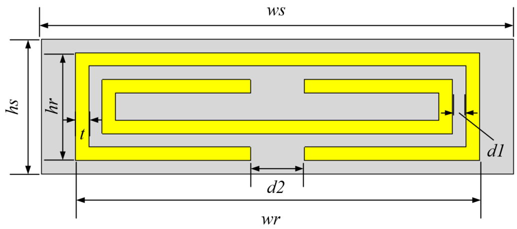


Fig. 1. Geometry of the proposed decoupling baffle.

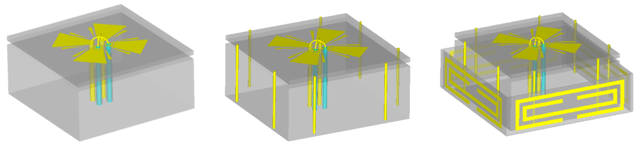

(a) (b) (c)

Fig. 2. Configurations of (a) original antenna unit, (b) modified antenna unit and (c) antenna with four SRR-loaded baffles.

Fig. 3 illustrates the transverse magnetic field between the baffle and the dielectric block. The dielectric block beneath the dipole arms can be approximately regarded as a perfect magnetic conductor (PMC) at the boundary of its four sidewalls, thus magnetic fields at the boundary are orthogonal to the sidewalls (and the SRR baffles) and, therefore, can effectively excite the SRR [21]. Fig. 4 shows the transmission coefficients of the single SRR-loaded baffle at different polarization angles from 0° to 60°. It can be clearly seen that, except at the 0° polarization angle, the transmission coefficients are below -15 dB in the 5G band of 3.4-3.8 GHz. This explains why SRR-loaded baffle can significantly suppress the coupling wave. As the decoupling baffles also form an open cavity, it tends to increase the operating frequency of the antenna unit.

To enhance the bandwidth and the impedance matching, eight vertical metal cylinders are added (cf. Fig. 2 (b)), which act as inductive loading to counteract the capacitive reactance of the antenna unit. The dimensions of the proposed decoupling baffle are tuned by considering both mutual coupling reduction and impedance matching.

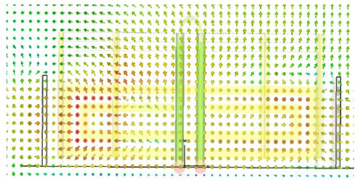

Fig. 3. Magnetic field between the baffle and the dielectric block at 3.6 GHz.

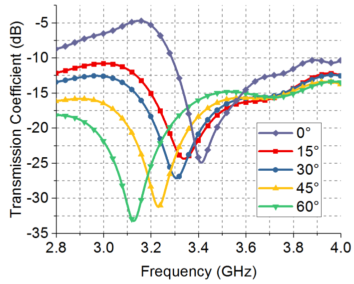


Fig. 4. Transmission coefficients of the proposed SRR-loaded baffle.

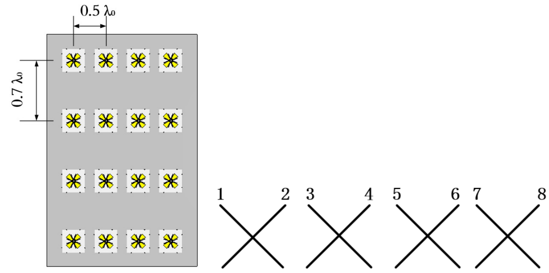


Fig. 5. (a) Configuration of a typical BS array; (b) port numbers of a 1×4 array.

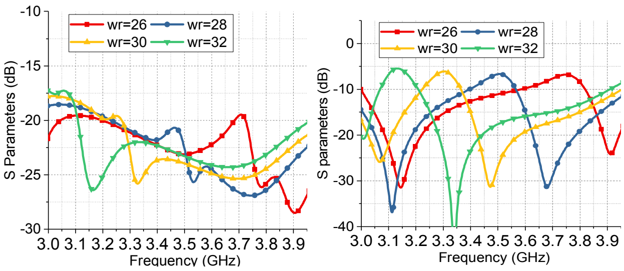


(a) (b)

Fig. 6. Simulated results of (a) S36 and (b) S33 when $wr$ varies.

In a typical BS array, the vertical element spacing is usually more significant than the horizontal element spacing because the elevation scanning range is much smaller than the horizontal scanning range [23], [24]. Hence, the worst mutual coupling is mainly attributed to the coupling between neighboring horizontal elements. Fig. 5 (a) shows a typical configuration of the BS array. Since the vertical spacing is sometimes even larger than 0.7$\lambda_0$ (where $\lambda_0$ is the free-space wavelength at the center frequency), the coupling between elements in different rows is much weaker than that between elements in the same row. Therefore, a horizontal 1×4 array with 0.5$\lambda_0$ inter-element spacing is a good example to demonstrate the proposed decoupling technique for BS arrays.

This article has been accepted for publication in a future issue of this journal, but has not been fully edited. Content may change prior to final publication. Citation information: DOI 10.1109/LAWP.2020.3020855, IEEE Antennas and Wireless Propagation Letters



The port numbering of the 1×4 array is given in Fig. 5 (b).

Fig. 6 shows the simulated S-parameters as the outer ring width, *wr*, varies. For brevity, only S36 and S33 are shown. From the parameter study, the center of the stopband should be out of the operating band, and the -15dB matching level should not be degraded. Considering the decoupling performance and the bandwidth, the optimized dimensions of the baffle are given as *ws = 35 mm, hs = 10 mm, wr = 30 mm, hr = 8 mm, d2 = 4 mm, d1 = 1 mm, t = 1 mm* (cf. Fig. 1). Note that the baffle height is less than the antenna height. Thus, the baffles do not affect the antenna profile, which is highly desirable for BS arrays.

## III. MIMO Array with Loaded Baffles

### A. Array Configuration

The configuration of a 1×4 array with 0.5 $\lambda_0$ inter-element spacing is shown in Fig. 7. It is noted that the ground plane is upturned at its edges, which helps slightly in improving the mutual coupling of the outer antenna elements (i.e., the first and last array elements). Also, note that the upturned ground edges can be made for each row in a sizeable planar BS array. The 1×4 array with loaded baffles is fabricated. A photo of the prototype is shown in Fig. 7 (c).

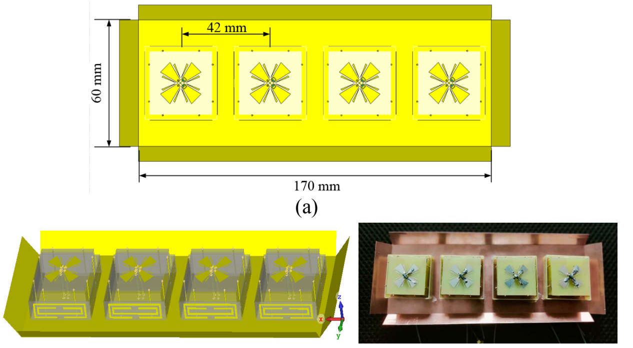


Fig. 7. Geometry of the 1× 4 array. (a) Top view, (b) perspective view, and (c) photo of the prototype.

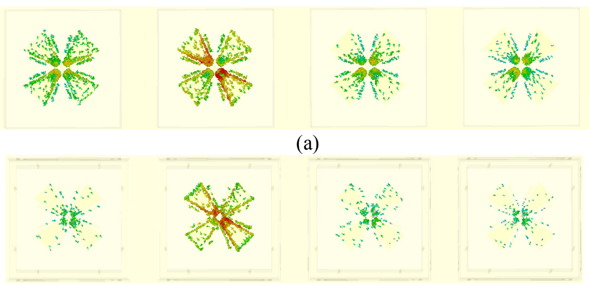


Fig. 8. Surface current distributions of (a) original array and (b) decoupling array when port 3 is excited.

### B. Simulated and Experimental Results

To illustrate the decoupling principle, the surface current distributions of the radiating patches of the original array and the decoupling array when Port 3 is excited are shown in Fig. 8 (a) and (b), respectively. It can be clearly seen that the induced surface currents of the decoupling array are effectively suppressed thanks to the SRR-loaded baffles. For better illustration and due to the symmetry of the array, only parts of the S-parameters are presented. Also, S-parameters less than -30 dB are omitted. Fig. 9 (a) shows that the reflection coefficient maintains -15 dB from 3.4 GHz to 3.8 GHz. The polarization isolation of the antenna unit is over 25 dB, as shown in Fig. 9 (b).

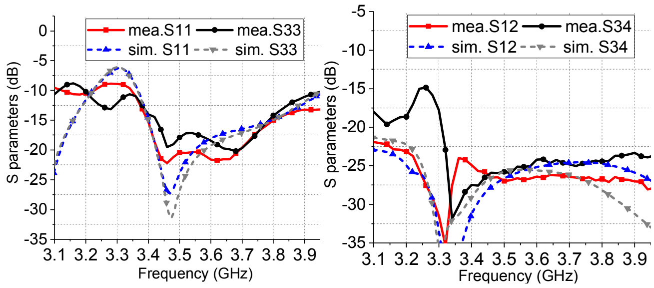


Fig. 9. Simulated and measured S-parameters of the first and second elements of the proposed array. (a) reflection coefficients of first and second elements and (b) isolation between the ports of each element.

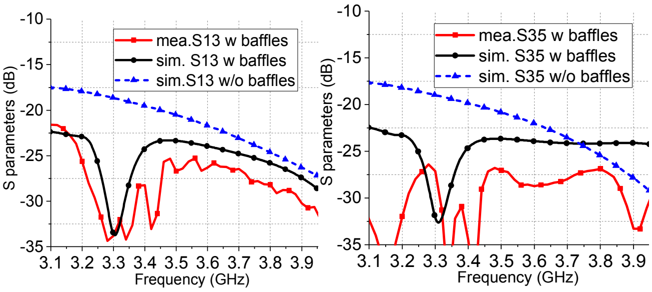


Fig. 10. Simulated and measured S-parameters between the co-polarized ports of the array. (a) S13, and (b) S35.

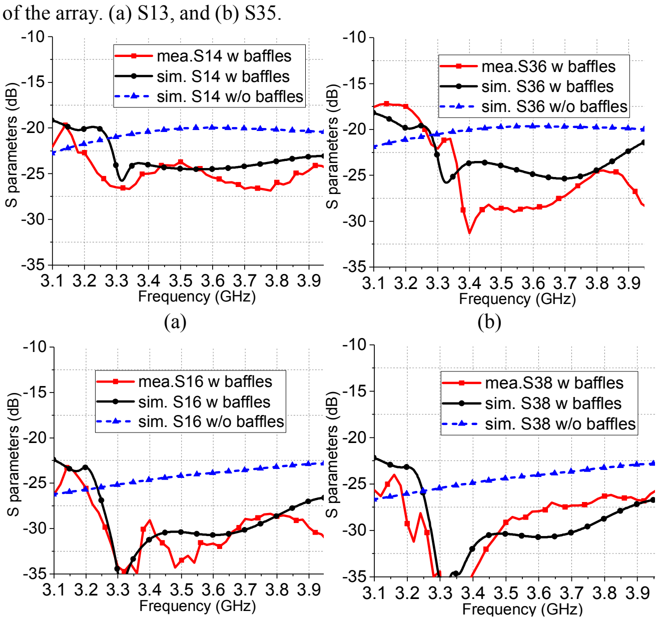


Fig. 11. Simulated and measured S-parameters of the cross-polarization between the array elements. (a) ports of first and second elements, S14, (b) second and third elements S36, (c) ports of first and third elements, and (d) ports of second and third elements S38.

The coupling between co-polarized elements is depicted in Fig. 10 (a) and (b). As can be seen, S13 and S35 gradually decrease as the frequency increases. Thus, reducing the

This article has been accepted for publication in a future issue of this journal, but has not been fully edited. Content may change prior to final publication. Citation information: DOI 10.1109/LAWP.2020.3020855, IEEE Antennas and Wireless Propagation Letters



low-frequency coupling is the main task. Measured results show that all the co-polarization coupling is below -25 dB in the operating band. Compared with co-polarization coupling, the coupling between cross-polarized elements (i.e., cross-polarization coupling) in the proposed array is somewhat stronger. These kinds of couplings (e.g., S14 and S36) are more difficult to reduce [2] in that they are strongly determined by the capacitive couplings between the ends of cross-polarized dipole arms (see Fig. 6 (b)). Nevertheless, it is shown that the proposed loaded baffles can effectively reduce such kind of coupling. Fig. 11 (a) and (b) demonstrate the cross-polarization decoupling performance between the adjacent elements of the first and second element given by S14 and S36 are reduced by 5 dB and the cross-polarization coupling between first and third elements indicated by S16 and S38 are reduced below -27 dB, as shown in Fig. 11 (c) and (d).

Following the assumptions in [2], active VSWR is used to demonstrate the decoupling effect. Assuming the 1×4 array (with and without the decoupling baffles) is used to serve two users simultaneously in a Rayleigh fading environment using zero-forcing (ZF) precoder, Fig. 12 depicts the worst active VSWRs of the eight antenna ports for 50 random snapshots. As can be seen, the active VSWR is significantly suppressed using the decoupling baffles.

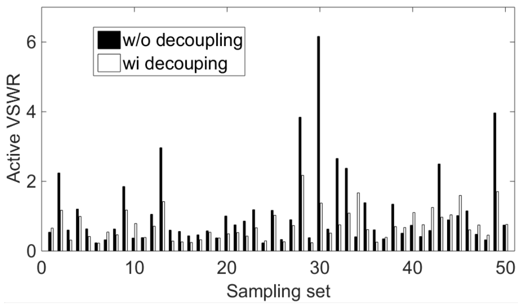


Fig. 12. Comparison of the active VSWR of the 1 × 4 array with (wi) and without (w/o) decoupling baffles.

The influence of the loaded baffles on the radiation performance of the antenna is also investigated. Due to the page limit, only the 3.6-GHz simulated and measured radiation patterns in the horizontal (H) and vertical (V) planes for elements 1, 2, 3, and 4 are plotted in Fig. 13. As mentioned in the introduction, the horizontal array is for MIMO application. Thus, only the radiation patterns of individual elements are presented here. The simulated gains of the antenna with and without decoupling structures are almost the same. The measured gains of elements 1, 2, 3 and 4 are 5.5 ± 0.5 dBi, 6.1 ± 0.5 dBi, 5.6 ± 0.6 dBi and 5.6 ± 0.6 dBi, respectively, in the whole band. The measured HPBWs of elements 1, 2, 3, and 4 in the H-plane are 75 ± 5°, 77 ± 5°, 91 ± 10°, and 85 ± 10°, respectively, in the operating band, while the measured HPBWs of all the elements in the V-plane are 75± 5°. Thus, the gain and HPBW do not have large fluctuation as the frequency varies. The small discrepancies between the simulated and measured results are mainly due to manufacturing tolerance, imperfect soldering, and measurement errors.

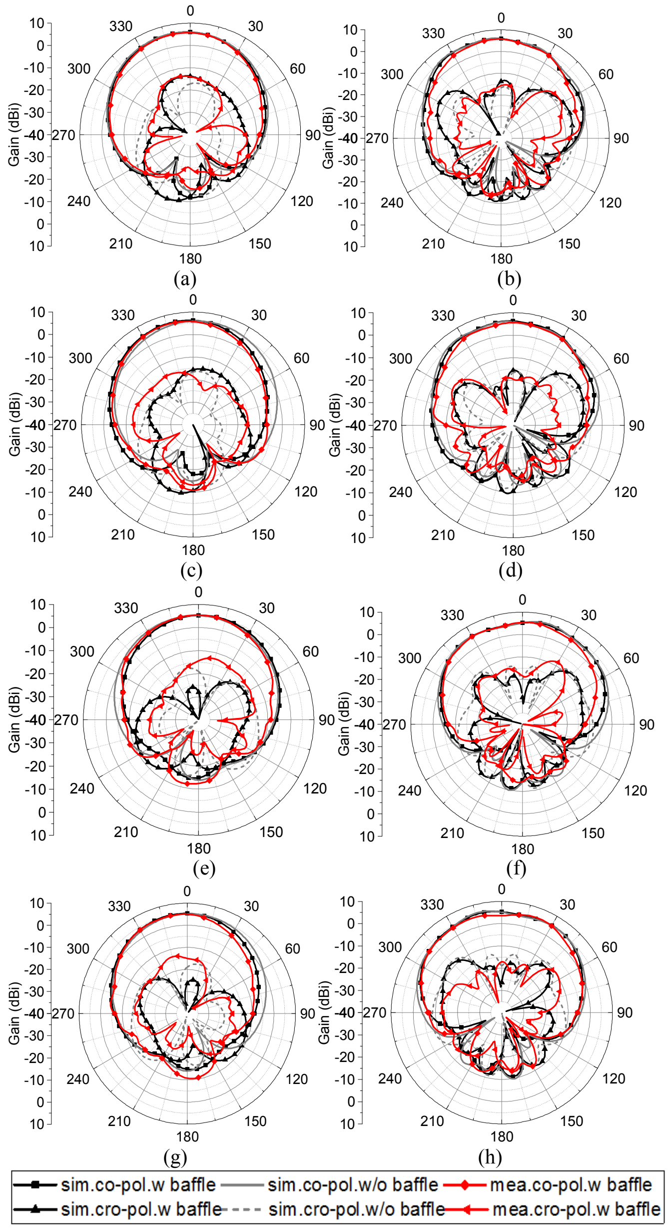


Fig. 13. Simulated and measured radiation patterns at 3.6 GHz: (a) V-plane of Port 1, (b) H-plane of Port 1, (c) V-plane of Port 2, (d) H-plane of Port 2, (e) V-plane of Port 3, (f) H-plane of Port 3, (g) V-plane of Port 4, and (h) H-plane of Port 4.

## IV. Conclusions

In this letter, decoupling baffles loaded by SRR have been designed and used with a dually-polarized array of 1×4 cross-dipoles. Simulated and measured results have been used to verify the proposed decoupling method. Simulation results have an excellent agreement with the measurement results. The mutual coupling of the array has been reduced to be below -25 dB in the 5G band of 3.4-3.8 GHz while maintaining proper impedance matching and radiation performance. Compared with previous work, the proposed decoupling baffle is a simple structure which can effectively reduce both co- and cross-polarization coupling in 5G massive MIMO array without increasing the antenna profile.

## REFERENCES


[1] A. Zaidi, F. Athley, J. Medbo, et al., *5G Physical Layer: Principles, Models and Technology Components*, Academic Press, 2018.

[2] K.-L. Wu, C. Wei, X. Mei, and Z. Zhang, "Array-antenna decoupling surface," *IEEE Trans. Antennas Propag.*, vol. 65, no. 12, pp. 6728-6738, Dec. 2017.

[3] X. Chen, S. Zhang, Q. Li, "A review of mutual coupling in MIMO systems," *IEEE Access*, vol. 6, pp. 24706 - 24719, 2018.

[4] S. Zhang, et al., "Mutual coupling suppression with decoupling ground for massive MIMO antenna arrays," *IEEE Trans. Veh. Technol.*, vol. 68, no. 8, pp. 7273-7282, Aug. 2019.

[5] H.-H. Sun, C. Ding, H. Zhu, and Y. J. Guo, ''Dual-polarized multiresonance antennas with broad bandwidths and compact sizes for base station applications,'' *IEEE Open J. Antennas Propag*., vol. 1, pp. 11–19, 2020.

[6] C. Ding, H. Sun, H. Zhu, and Y. J. Guo, "Achieving Wider Bandwidth With Full-Wavelength Dipoles for 5G Base Stations," *IEEE Trans. Antennas Propag.*, vol. 68, no. 2, pp. 1119-1127, Feb. 2020.

[7] M. A. Al-Tarifi, M. S. Sharawi, and A. Shamim, "Massive MIMO antenna system for 5G base stations with directive ports and switched beam steering capabilities," *IET Microwaves Antennas & Propag.*, vol. 12, pp. 1709-1718, Aug. 2018.

[8] M. Abdullah, et al., "Mutual coupling and correlation of closely spaced patch antennas," *Electron. Lett.*, vol. 55, no. 13, pp. 724–726, 2019.

[9] M. Li, B. Zhong, and S. W. Cheung, "Isolation enhancement for MIMO patch antennas using near-field resonators as coupling-mode transducers," *IEEE Trans. Antennas Propag.*, vol. 67, no. 2 pp. 755-764, Feb. 2019.

[10] Z. Wang, C. Li, and Y. Yin, "A meta-surface antenna array decoupling (MAAD) design to improve the isolation performance in a MIMO system," *IEEE Access*, vol. 8, pp. 61797-61805, 2020.

[11] Z. Wang, C. Li, Q. Wu, and Y. Yin, "A metasurface-based low-profile array decoupling technology to enhance isolation in MIMO antenna systems," *IEEE Access*, vol. 8, pp. 125565-125575, 2020.

[12] I. Dioum, A. Diallo, S. M. Farssi, and C. Luxey, "A novel compact dualband LTE antenna-system for MIMO operation," *IEEE Trans. Antennas Propag.*, vol. 62, no. 4, pp. 2291–2296, Apr. 2014.

[13] C.-Y. Chiu, C.-H. Cheng, R. D. Murch, and C. R. Rowell, "Reduction of mutual coupling between closely-packed antenna elements," *IEEE Trans. Antennas Propag.*, vol. 55, no. 6, pp. 1732–1738, Jun. 2007.

[14] F. Yang and Y. Rahmat-Samii, "Microstrip antennas integrated with electromagnetic band-gap (EBG) structures: A low mutual coupling design for array applications," *IEEE Trans. Antennas Propag*., vol. 53, no. 4, pp. 2936–2946, Oct. 2003.

[15] H. S. Farahani, M. Veysi, M. Kamyab, and A. Tadjalli, "Mutual coupling reduction in patch antenna arrays using a UC-EBG superstrate," *IEEE Antennas Wireless Propag. Lett*., vol. 9, pp. 57–59, 2010.

[16] A. Habashi, J. Nourinia, and C. Ghobadi, "Mutual coupling reduction between very closely spaced patch antennas using low-profile folded split-ring resonators (FSRRs)," *IEEE Antennas Wireless Propag. Lett.*, vol. 10, pp. 862–865, 2011.

[17] S. Zhu, X. Yang, J. Wang, et al., "Mutual coupling reduction of ±45° dual-polarized closely spaced MIMO antenna by topology optimization," *IEEE Access*, vol. 8, pp. 29089-29098, 2020.

[18] H. Qi, L. Liu, X. Yin, H. Zhao, and W. J. Kulesza, "Mutual coupling suppression between two closely spaced microstrip antennas with an asymmetrical coplanar strip wall," *IEEE Antennas Wireless Propag. Lett.*, vol. 15, pp. 191–194, 2016.

[19] Y. Zhang, S. Zhang, J. Li, and G. F. Pedersen, "A transmission-line-based decoupling method for MIMO antenna arrays," *IEEE Trans. Antennas Propag*., vol. 67, no. 5, pp. 3117-3131, May 2019.

[20] J. Tang, et al., "A metasurface superstrate for mutual coupling reduction of large antenna arrays," *IEEE Access*, vol. 8, pp. 126859-126867, 2020.

[21] J. D. Baena, et al., "Equivalent-circuit models for split-ring resonators and complementary split-ring resonators coupled to planar transmission lines," *IEEE Trans. Microw. Theory Tech.*, vol. 50, no. 12, pp. 1451–1461, Apr. 2005.

[22] M. Li, X. Chen, A. Zhang, and A. A. Kishk, "Dual-polarized broadband base station antenna backed with dielectric cavity for 5g communications," *IEEE Antennas Wireless Propag. Lett.*, vol. 18, no. 10, pp. 2051-2055, Oct. 2019.

[23] X. Chen, S. Guo, and Q. Wu, "Link-level analysis of multiservice indoor distributed antenna system," *IEEE Antennas Propag. Mag.*, vol. 59, no. 3, pp. 154-162, Jun. 2017.

[24] R. He, Q. Li, B. Ai, *et al.*, "A Kernel-power-density based algorithm for channel multipath components clustering," *IEEE Trans. Wireless Commun.*, vol. 16, no. 11, pp. 7138 - 7151, Nov. 2017.